Full waveform inversion using blended acquisition geometry

Amsalu Y Anagaw, University of Alberta, Edmonton, Canada
aanagaw@ualberta.ca
and
M. D. Sacchi, University of Alberta, Edmonton, Canada

GeoConvention 2012:Vision

Summary

In frequency domain full-waveform inversion strategies, a finite set of discrete frequencies are selected and the inversion is carried out sequentially from low to high frequency data components. First, the long wavelength components of the model parameters are recovered from low frequency data, and then more details and features are extracted as the inversion proceeds with higher frequencies. In this paper, we investigate different frequency selection strategies on the solution of a matrix-free Gauss-Newton full waveform algorithm that uses simultaneous sources. We examine five strategies for frequency selection and test the performance of the algorithm with the BP/EAGE data set. Numerical results on the BP/EAGE model show that high fidelity results can be attained by inverting partially overl apped groups of temporal discrete frequencies.

Introduction

Full-Waveform inversion (FWI) is becoming part of our arsenal of methods for determining subsurface velocity models (Pratt et al., 1998; Virieux and Operto, 2009; Hu et al., 2011). The main objective of seismic waveform inversion is to retrieve the Earth model that best fits the observed seismic data. One of the main problems in FWI is the computational cost of the inversion for multiple sources and receivers. In addition, to avoid solutions that are trapped in local minima, one needs to provide a good initial velocity model or data with high-quality low frequency components. The computational cost of full waveform inversion is proportional to the number of sources of the experiment. This computational cost can be reduced by the use of simultaneous shooting techniques (Krebs et al., 2009; Ben-Hadj-Ali et al., 2011). The basic idea of the simultaneous shot method is to make super-shots by summing individual sources with a random encoding function (Romero et al., 2000). However, the simultaneous source technique introduces random cross-talk that arises from the correlation between shots. One way to reduce the cross-talk noise is by generating new random encoding supers-shots in every iteration (Krebs et al., 2009).

The full waveform inversion in frequency domain is carried out in a sequential approach starting from low to higher frequencies (group frequencies) (Sirgue and Pratt, 2004). The inversion obtained from the first group of frequencies is used to initialize the inversion for the next group and so on (Kim et al., 2011). We study various types of frequency grouping to solve the FWI problem in the case where the sources have been blended to gain computational efficiency. The frequency grouping strategies tested in this article are summarized in Table 1. We used a matrix-free Gauss-Newton full waveform algorithm with a simultaneous sources using a blended source encoding technique. On each iteration and frequency group, a new random encoding operator is generated. The robustness of the different frequency selection strategies on simultaneous encoded sources have been studied. Though all frequency selection strategies provide reasonable results, the partial overlapping group method demonstrates better result in terms of resolution and quality of the inverted model. Numerical results on BP/EAGE velocity model (Billette and Brandsberg-Dahl, 2005) are presented to illustrate the characteristics of the these strategies for simultaneous shot techniques in full waveform inversion.

Theory

Waveform inversion requires the minimization of the misfit or the object function; l_2 norm of residual between the observed data $\mathbf{d}^{obs}$ and the model data $\mathbf{d}^{cal}$

$$J(\mathbf{m}) = \frac{1}{2}\sum_{\omega\in\Omega_i} W_i \sum_{s,r}^{N_s,N_r} (\mathbf{d}^{cal}_{s,r}(\omega) - \mathbf{d}^{obs}_{s,r}(\omega))^{\dagger}(\mathbf{d}^{cal}_{s,r}(\omega) - \mathbf{d}^{obs}_{s,r}(\omega)) + \mu R(\mathbf{m}) \tag{1}$$

where † is the complex conjugate transpose, $R(\mathbf{m})$ is the regularization term, μ is the regularization parameter and, N_s and N_r represent the number of sources and receivers respectively, and W_i is the data weight for the simultaneous inversion of multiple frequencies (frequencies in a group). The variable Ω_i represents a group of frequency. We stress that the inversion of the first group (Ω_1) is initialized with a smooth model (starting model); the inversion with data from group Ω_{i+1} is initialized with the solution found by inverting group Ω_i. The objective function is minimized using Lagrangian constrained optimization method

$$\begin{aligned} &\underset{\mathbf{m}}{\text{minimize}} \quad J(\mathbf{m}) \\ &\text{subject to} \quad \mathbf{A}(\mathbf{m},\omega)\mathbf{p}_s(\omega) = \mathbf{f}_s(\omega), \end{aligned} \tag{2}$$

where $\mathbf{A}(\mathbf{m},\omega)$ is the forward modelling operator, which depends on frequency and the media properties, $\mathbf{p}_s(\omega)$ is the wavefield in space and $\mathbf{f}_s(\omega)$ is the source term. The modelled data is computed as $\mathbf{d}^{cal}_{s,r}(\omega) = \mathbf{r}\mathbf{p}_s(\omega)$, where $\mathbf{r}$ is a receiver operator. In the Gauss-Newton's minimization method, the reduced Gauss-Newton of the object function becomes

$$\mathbf{H}_{GN} = ((\nabla_{\mathbf{m}}\mathbf{A})\mathbf{p}_{\mathbf{s}})^{*}(\mathbf{A}^{*})^{-1}\mathbf{r}^{*}\mathbf{r}\mathbf{A}^{-1}(\nabla_{\mathbf{m}}\mathbf{A})\mathbf{p}_{\mathbf{s}} + \mu\nabla^2_{\mathbf{m}}R. \tag{3}$$

Then, the model perturbation update is computed iteratively using conjugate gradient method. The latter is equivalent to solving the following linear system of equations

$$\mathbf{H}_{GN}\triangle\mathbf{m} = -\mathbf{g}, \tag{4}$$

where $\mathbf{g}$ is the gradient of the objective function. In the Gauss-Newton method, we adopt the early termination of the conjugate gradient iteration and update the model parameters using a line search method. In the blended acquisition, super-shots are assembled using a random function as

$$\mathbf{S}(\omega)_{nsp} = \Gamma\mathbf{D}_{\mathbf{R}}\mathbf{f}_s(\omega) = \Psi\mathbf{f}_s(\omega), \tag{5}$$

where $\mathbf{S}(\omega)_{nsp}$ is a super-shot (*nsp*), Γ and $\mathbf{D}_R$ are the encoding function and randomization operator that randomly picks the monochromatic sources, respectively. The blending of shots in matrix form is given by

$$\Gamma(\omega,\tau) = [e^{-i\omega\tau_1} \quad e^{-i\omega\tau_2} \quad e^{-i\omega\tau_3} \quad ... \quad e^{-i\omega\tau_{ns}}]^T, \tag{6}$$

where τ_i is a random time delay randomly chosen in the interval $[0,t]$ and t is the maximum time delay. Making use of the above equation, the forward problem becomes $\mathbf{p}^{cal}_{nsp}(\omega) = \mathbf{A}(\mathbf{m},\omega)^{-1}\Psi\mathbf{f}_s(\omega)$.

Examples

Figure 1 [a] and [b] are the true BP/EAGE velocity model and the initial linearly increasing velocity model with velocity increasing from 1400 m/s to 4000 m/s, respectively. First, we generated synthetic data with a total number of 225 sources and 338 receivers. For inversion, a set of nine discrete frequencies were selected (0.18, 0.21, 0.40, 0.63, 1.00, 1.61, 3.04, 4.00 and 4.64 Hz). In order to recover the long wavelength components of the velocity model, one has to start the inversion from

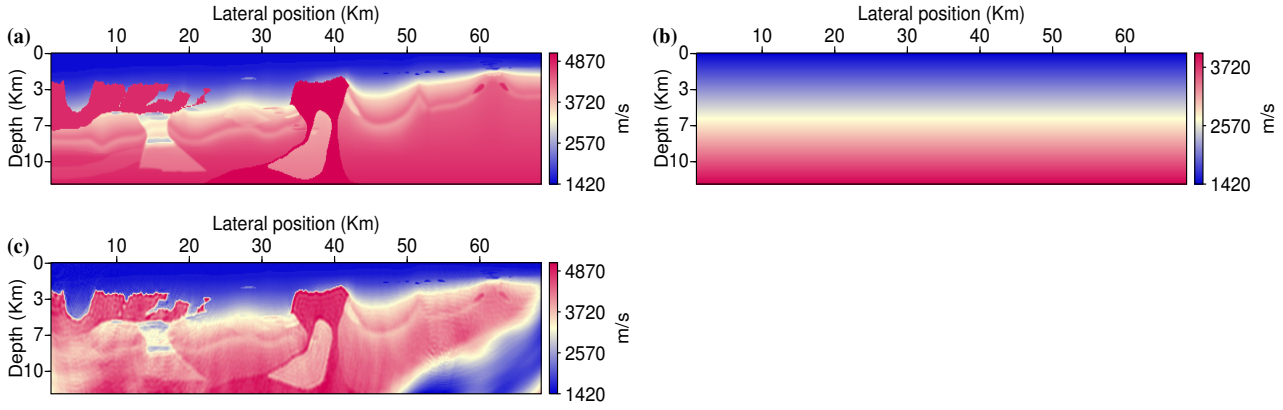

Figure 1 *BP/EAGE velocity velocity mode (a), linearly increasing velocity model with depth used as starting model for inversion (b) and reconstructed velocity mode using a sequential single discrete frequency with a conventional shot gathers technique (c).*

a very low frequency data Hu et al. (2011). The waveform inversion is then carried out sequentially from low to high frequency data groups. All frequencies within one group are simultaneous inverted. In each frequency group inversion, the lower frequency data components were given more weight than the next frequency data component via the function W_i. For each frequency group, we compute a maximum of 30 Gauss-newton iterations. Table 1 summarizes all the frequency groups. Figure 1 [c] is the reconstructed velocity model using the sequential single discrete frequencies approach without blending the sources. Figure 2 [a-e] are the reconstructed velocity model using different fre-

Table 1 *Frequency selection strategies for FWI.*

Group	Individual	Overlap	Partial overlap	Simultaneous
Ω_1	f_1, f_2, f_3	f_1, f_2, f_3	f_1, f_2, f_3, f_4	f_1, f_2, f_3, f_4, f_5, f_6, f_7, f_8, f_9
Ω_2	f_4, f_5, f_6	f_1, f_2, f_3, f_4, f_5	f_3, f_4, f_5, f_6	
Ω_3	f_7, f_8, f_9	f_1, f_2, f_3, f_4, f_5, f_6, f_7	f_5, f_6, f_7, f_8	
Ω_4		f_1, f_2, f_3, f_4, f_5, f_6, f_7, f_8, f_9	f_7, f_8, f_9	

quency selection strategies for FWI using simultaneous monochromatic blended sources. We used a total of 23 super-shots where each super-shot is constructed by randomly encoding 10 monochromatic sources. In every frequency group, a new random source is generated. In addition, on every iteration, a new blending operator is generated with a maximum time delay of 1.5 sec. Though all frequency selection strategies provide reasonable results, the individual and partial overlap grouping methods demonstrate better result in terms of resolution and quality of the inverted model. In order to compare the quality of our results, we compute $Q = 10\log_{10}[||\mathbf{m}_{true}||^2/||\mathbf{m}_o - \mathbf{m}||^2]$ as our comparison metric, where $\mathbf{m}_{true}$ and $\mathbf{m}$ are the true velocity model and reconstructed velocity model, respectively. The reconstructed velocity models are shown in Figure 2. These numerical inversion results reproduces results that are comparable to the original velocity model. Clearly, the best resolved result was achieved with a partially overlapping frequency strategy ($Q = 41.54dB$). The inversion utilizing simultaneous shots provides models which are in close agreement to the one obtained using the a single shot data inversion method, see Figure 1 and 2. The salt body structures and the shallow anomalies are properly reconstructed. However, all methods are struggling to reconstruct the deep part on the right side of the model.

Conclusion

Using the advantage of simultaneous sources technique, we are able to show results that are comparable with the conventional acquisition data sets. The full waveform inversion algorithm is based

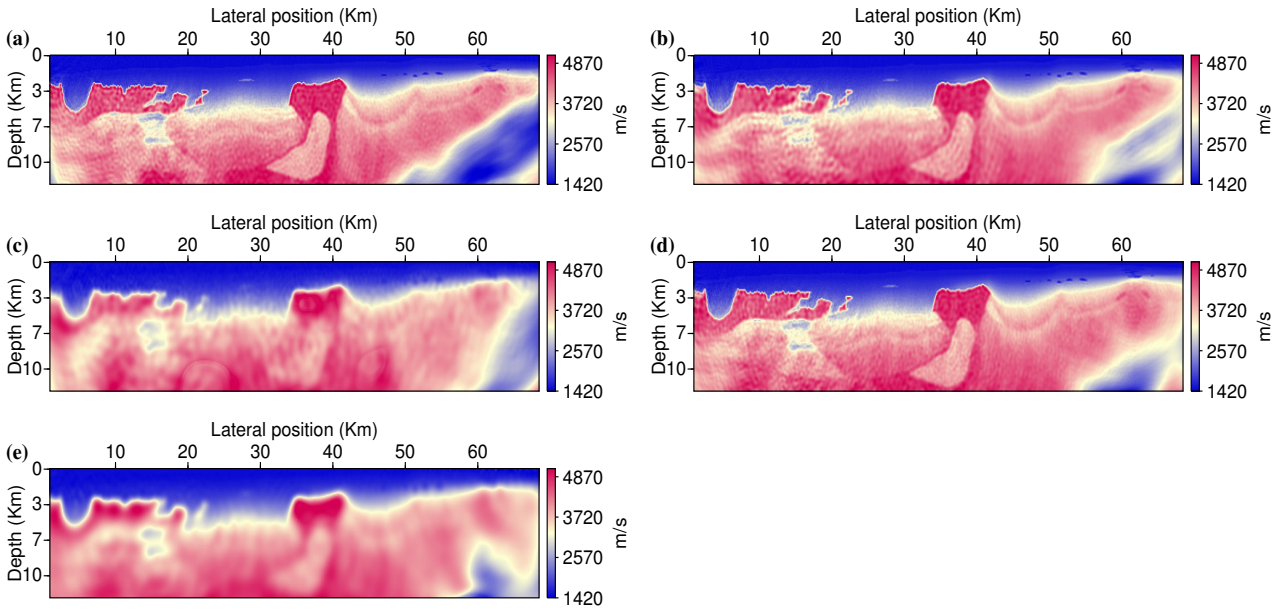

Figure 2 *Reconstructed velocity mode using simultaneous encoded sources. Reconstructed velocity model using a sequential single discrete frequencies method (a), reconstructed model using individual group (b), overlap group (c), partial overlap group (d) and simultaneous methods (e). Quality factors for (b), (c), (d), (e) and (f) are Q = 31.24, 38.79, 37.71, 41.54 and 37.87, respectively.*

on a quadratic matrix-free Gauss-Newton method. Different frequency selection strategies have also be studied to examine the robustness of the method in terms of quality and resolution of the inverted model parameters. In this particular example, we have found that partially overlapping discrete frequencies groups provided the best inverted velocity model.

Acknowledgements

The authors are grateful to the sponsors of Signal Analysis and Imaging Group (SAIG) at the University of Alberta.

References

Ben-Hadj-Ali, H., S. Operto, and J. Virieux, 2011, An efficient frequency-domain full waveform inversion method using simultaneous encoded sources: Geophysics, **76**, R109–R124.

Billette, F. and S. Brandsberg-Dahl, 2005, The 2004 BP velocity benchmark., *in* 67th Annual Internat. Mtg., EAGE, Expanded Abstracts, B035. EAGE.

Hu, W., A. Abubakar, T. M. Habashy, and J. Liu, 2011, Preconditioned non-linear conjugate gradient method for frequency domain full-waveform seismic inversion: Geophysical Prospecting, **59**, 477–491.

Kim, Y., H. Cho, D.-J. Min, and C. Shin, 2011, Comparison of frequency-selection strategies for 2d frequency-domain acoustic waveform inversion: Pure and Applied Geophysics, **168**, no. 10, 1715–1727. 10.1007/s00024-010-0196-8.

Krebs, J. R., J. E. Anderson, D. Hinkley, R. Neelamani, S. Lee, A. Baumstein, and M.-D. Lacasse, 2009, Fast full-wavefield seismic inversion using encoded sources: Geophysics, **74**, WCC177–WCC188.

Pratt, G., C. Shin, and Hicks, 1998, Gauss−newton and full newton methods in frequency−space seismic waveform inversion: Geophysical Journal International, **133**, 341–362.

Romero, L. A., D. C. Ghiglia, C. C. Ober, and S. A. Morton, 2000, Phase encoding of shot records in prestack migration: Geophysics, **65**, 426–436.

Sirgue, L. and R. Pratt, 2004, Efficient waveform inversion and imaging: A strategy for selecting temporal frequencies: GEOPHYSICS, **69**, 231–248.

Virieux, J. and S. Operto, 2009, An overview of full-waveform inversion in exploration geophysics: Geophysics, **74**, WCC1–WCC26.